Toward a Unified Framework for Modeling and Analysis of Diversity in Joint Source-Channel Coding

Andres Kwasinski, *Member, IEEE*, and K. J. Ray Liu, *Fellow, IEEE*

***Abstract*— The study of Joint Source-Channel Coding (JSCC) systems faces one major challenge in obtaining an analytical expression for the function that links end-to-end distortion with channel signal-to-noise ratio, the D-SNR curve. In this paper, for certain multimedia systems using practical source and channel codes in a JSCC bit rate allocation design, the D-SNR curve is shown to be well approximated by a set of carefully selected points where the relative contribution of channel errors to end-to-end distortion is small. This approach has the potential advantage that it could be applied to represent performance of many practical systems using JSCC bit rate allocation for which it is shown that the D-SNR function is approximately linear in log-log scales. A unified framework for the modeling, analysis and performance measurement of these systems is proposed by considering a view of diversity more general than its usual interpretation. This view extends that of diversity to include redundant information so coding and diversity gain are still used to characterize performance. Furthermore, the proposed approach is applied to study issues arising from using practical source and channel codes, including the effects on performance of channel codes of different strength or source codes with different compression efficiency.**

***Index Terms*— Adaptive coding, source coding, channel coding.**

I. Introduction

ONE of the most challenging problems in wireless communications is the need to overcome channel fading. One solution is the use of diversity, which improves the link quality by transmitting multiple copies of the signal in a way that each is independently affected by the channel. Performance is usually characterized in terms of the error rate at high signal-to-noise ratios (SNRs), where the error rate-SNR function exhibits a linear behavior in log-log scales. Consequently, performance is represented using two magnitudes: the *"coding gain"* and the *"diversity gain"* [1]. Diversity is not exclusive to implementations at the physical layer. As studied in [2], diversity can also be formed when multiple channels are provided to the application layer, where they are exploited through multiple description source codecs or joint source-channel coding (JSCC). In this case, performance is measured through the source distortion and diversity is quantified through a magnitude akin to the diversity gain named "distortion exponent". In this sense, diversity shows an overlap with the concept of redundancy because it is partially generated as redundancy from the coding processes.

In this paper, we approach the concept of diversity with a more general view than the one limited to the presence of multiple channels or fading. In essence, the concept of diversity, as that of transmitting multiple copies of a message, can be extended to include the notion of redundant information. In fact, error correcting codes exhibit an inherent diversity since (maybe partial) copies of the message are coded as parity data of a channel code. Also, residual redundancy after source encoding can be seen as diversity in the form of useful partial information. Then, since redundancy can be seen as a form of diversity, we argue that they can both be explored in a unified way. In this paper we explore this concept for certain classes of real-time multimedia systems that use JSCC bit rate allocation, which is the distribution of a fixed transmit bit rate budget between source and channel coding [3], [4].

Designs based on JSCC had been the subject of much research since they can improve performance when Shannon's separation principle [5], [6] does not hold; i.e., in cases, such as transmission of real-time multimedia, where the assumptions of arbitrary large source code dimension, arbitrary long channel code blocks, and infinite complexity and delay, do not hold. There are many JSCC techniques, encompassing digital, analog and hybrid digital-analog (HDA) implementations. Among the not all-digital techniques, many are built on the idea of designing mappings from the source space into the channel space. While for the analog JSCC techniques the mapping is direct [7], [8] or through processing (iterations) over a non-linear state space [9], in HDA techniques there may be a quantization step that is applied to the source samples [10], [11], [12], [13]. Another possible HDA technique sends the coded source over two streams: a quantized and a an analog stream [14], [15], [16], [17]. Many of the digital techniques are reviewed in [3], [4], where they are separated between integrated source-channel coders [18] and joint designs of tandem source and channel codecs. This later category is further divided in channel optimized quantization [19], index assignment [20], unequal error protection techniques [21] and joint bit rate allocation. Our present work is focused on this later technique. Due to the large body of research in this area we highlight only the representative works [22] for speech

Paper approved by M. Skoglund, the Editor for Source/Channel Coding of the IEEE Communications Society. Manuscript received December 29, 2005; revised June 20, 2006, January 18, 2007, and June 22, 2007.

A. Kwasinski is with Texas Instruments Inc., Germantown, MD (e-mail: akwasinski@ieee.org).

K. J. Ray Liu is with the Department of Electrical and Computer Engineering, University of Maryland, College Park, MD (e-mail: kjrliu@umd.edu).

Digital Object Identifier 10.1109/TCOMM.2008.050670.

Fig. 1. Block diagram of the system under study

transmission in mobile channels, [23] for image transmission and [24] for video communication.

One of the problems when studying JSCC bit rate allocation is that it is not possible to obtain closed form solutions for the D-SNR curves [25], which are those functions relating end-to-end distortion with channel SNR. This is because generally the design is based on iterative methods [26], [27], [28], [29] or on exhaustive search over reduced spaces [30]. A simple solution is to assume that the source is encoded optimally and transmitted at a rate equal to the channel capacity. This results in the OPTA (optimum performance theoretically attainable) curve [31]. In [32], [33], performance bounds are developed by resorting to high and low SNR approximations, error exponents, asymptotically large source code dimension, and infinite complexity and delay. These works are the first ones to suggest the D-SNR relation of the type discussed in the present work but, by their own nature, they cannot answer questions arising in more practical designs such as if performance can still be characterized in the same way, and how it will change depending on the source and channel codes being used. Still following an information theoretic approach based on outage capacity formulation, [2] studied the concept of *Source-Channel Diversity* in its traditional form, i.e. considering parallel channels and behavior at arbitrary large SNR. In an effort to model the D-SNR curve of video signals with practical channel codes, in [34] a model is selected from several candidates by choosing the best fit to measured data. Interestingly, the chosen model is the only one that shows similarity with the one we will show to be correct for a certain class of practical JSCC systems.

Our main contribution is the modeling of JSCC bit rate allocation D-SNR curves for practical source and channel codes. We accurately approximate the D-SNR curve by using a set of carefully selected points, which are those where the relative contribution of channel errors to end-to-end distortion is fixed and small. We show through this that end-to-end distortion, D, and channel SNR, γ, are related approximately through a function $D \approx (G_c\gamma)^{-10m}$. This is the same relation between error rate and arbitrary large SNR as in systems with channel fading. Recognizing this and resorting to the expanded view of diversity, we propose a unified framework for the modeling, analysis and performance measurement of multimedia systems that uses two magnitudes: the coding gain G_c (the translation along the axis of SNR in dBs) and diversity gain m (the slope and, physically, the amount of redundancy), which we choose instead of distortion exponent so as to provide a unified view.

The approach followed to characterize the D-SNR curve will be demonstrated to be simple and accurate in representing the behavior of some important practical source and channel codes without resorting to information-theoretic or asymptotic analysis. This considers the constraints of practical real-time multimedia communications, where delay limits the use of ARQ techniques and channel errors have to be constrained for the error concealment to be effective. This constitutes a new viewpoint for the study of these systems which readily provides important design information such as the performance difference with ideal information-theoretical bounds, quantitative results of how performance changes when using stronger channel codes or less efficient source codecs and the difference in performance behavior between using block and convolutional codes. Finally, to illustrate how the proposed approach can be applied in practice, we study a CDMA network carrying speech calls encoded with the GSM-AMR codec and distortion measured with the perceptually-based PESQ standard.

This paper is organized as follows: In Section II, we describe the problem of JSCC bit rate allocation. Section III characterizes the D-SNR curves for a certain class of source-channel coding schemes, and discusses some practical considerations. Section IV applies the proposed model to assess the impact of the source codec and channel codecs on performance and to characterize a practical speech communication system over CDMA. Finally, Section V summarizes conclusions and contributions.

II. The Problem of Joint Source-Channel Bit Rate Allocation

Consider a simplified communication system as in Figure 1. We assume that the system transmits a real time (subject to strict delay constraint) source for which end-to-end distortion is the relevant performance measure. Unless stated otherwise, distortion will be measured using the mean squared error. In each transmission period the system inputs N memoryless source samples. These samples are successively source encoded, channel encoded, transmitted over an additive white Gaussian (AWGN) channel with signal-to-noise ratio (SNR) γ, and decoded at the receiver.

The source samples are first encoded in a single description source encoder at a rate of x bits per source sample. The distortion-rate (D-R) function measures the codec performance. For well-designed codecs, the D-R function is convex and decreasing, and can be frequently considered to be of the form

$$D_S(x) = \mu\, 2^{-2\nu x}, \tag{1}$$

since it can approximate or bound a wide range of practical systems such as an MPEG-like video codec [35], [36], a CELP-type speech codec [37], or when the high rate approximation holds [2]. The output of the source encoder, which we call a "source block", is processed in a channel encoder at a rate r. The codewords at the output of the channel encoder are organized into a frame and transmitted at a fixed transmit bit rate W bits/frame using BPSK modulation.

The design goal is, given the channel SNR, to jointly set source and channel coding rates so as to minimize the end-to-end distortion while not exceeding the total transmit bit rate. The end-to-end distortion is formed by the source encoder distortion (which depends on the source encoding rate) and the channel-induced distortion (which depends on the channel SNR, error protection scheme, channel coding rate and error concealment operations). Typically both the source and the channel coding rates are chosen from a finite set. Each combination of a source and a channel coding rate is an operating mode, which we denote as Ω_i. We will denote the set of all operating modes by $\Omega = \{\Omega_i\}$. Source and channel coding rate are related to the transmit bit rate through the relation $W \geq Nx/r$. Based on this, the problem of JSCC bit rate allocation can be stated as

$$\min_{\Omega} \Big\{ D_F P_{\Omega_i}(\gamma) + D_S(\Omega_i)\Big(1 - P_{\Omega_i}(\gamma)\Big)\Big\}, \qquad (2)$$

where $D_S(\Omega_i)$ and $P_{\Omega_i}(\gamma)$ are, respectively, the source codec D-R function and the frame error probability for the operating mode Ω_i, and D_F is the distortion when the frame is received with errors and the lost data has to be replaced through error concealment at the source decoder. The solution to (2) is the operating mode that yields the minimum end-to-end distortion for a given channel SNR. When considering a range of channel SNRs, the solutions of (2) form a minimum distortion-channel SNR function, which we call the *"D-SNR curve"*. Most available operating modes do not form part of the solutions of (2). To be part of the solution that minimizes end-to-end distortion, the channel coding rate for a given source encoding rate has to be chosen as the smallest possible one such that the relation $W \geq Nx/r$ is as close as possible to an equality. In practice, some bit padding of the frame is necessary because the discrete number of choices for source and channel coding rate prevent achieving an exact equality in $W \geq Nx/r$. Good and efficient designs minimize the amount of padding. In fact, operating modes that use inefficient amounts of bit padding tend to form a small part of the D-SNR curve, if any, because they are quickly outperformed by more efficient modes. In order to simplify the presentation, we will use these facts to ignore frame bit-padding and approximate $W \approx Nx/r$, i.e. Ω can be described by the enumeration of any one of the available source or channel coding rates.

III. Source-Channel Diversity in JSCC Bit Rate Allocation

Let $d_{\Omega_i}(\gamma) = D_F P_{\Omega_i}(\gamma) + D_S(\Omega_i)\big(1 - P_{\Omega_i}(\gamma)\big)$, as per (2), be the D-SNR characteristic of a single operating mode. We call $d_{\Omega_i}(\gamma)$ the *single-mode D-SNR curve*. Figure 2 (which was created using a family of Rate Compatible Punctured Convolutional -RCPC- codes [38], [39] and source coding D-R function as in (1) with $\mu = \nu = 1$) shows the single-mode D-SNR curves that are active in the solution of the JSCC bit rate allocation problem, as well the envelope formed by these curves, which is the D-SNR curve. The comparison of two single-mode D-SNR curves shows the basic tradeoff associated with JSCC bit rate allocation. Let's consider that the indexes of the operating modes are sorted in increasing source encoding rate order; i.e. $i > j$ (from Ω_i and Ω_j) if $x_i > x_j$.

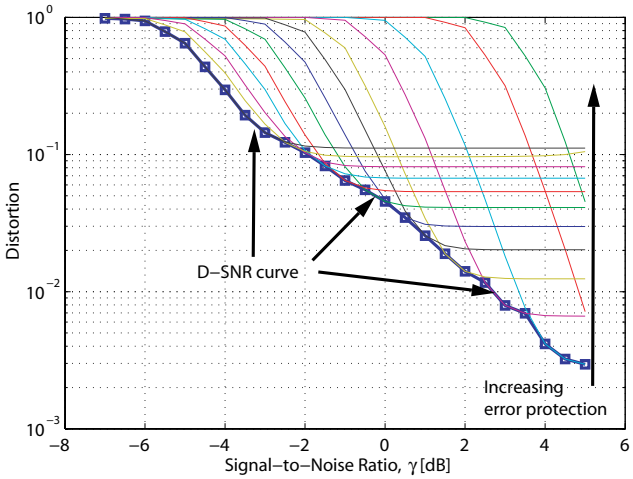

Fig. 2. Single mode D-SNR curves and the solution to the problem of joint source-channel bit rate allocation.

Following $W \approx Nx/r$, $i > j$ also means that $r_i > r_j$. For each single-mode D-SNR curve the distortion only increases due to channel errors because source and channel coding are fixed. Then, the single-mode D-SNR curve is practically a constant equal to $D_S(\Omega_i)$ for as long as the SNR is high enough for the channel code to correct most of channel errors. Clearly, over the section where two single-mode D-SNR curve are approximately constant, the one with a larger source encoding rate will present lower distortion because $D_S(\Omega_j) > D_S(\Omega_i)$ for $i > j$. Let γ_i^* be the SNR value at which the distortion of the mode-Ω_i single-mode D-SNR curve starts to noticeably increase. For well-behaved channel codes and $i > j$, we have that $\gamma_i^* > \gamma_j^*$ because $r_i > r_j$, i.e. channel errors start to become significant at a higher SNR for weaker channel codes. The overall effect is that for two curves $d_{\Omega_i}(\gamma)$ and $d_{\Omega_{i+1}}(\gamma)$, we have $d_{\Omega_{i+1}}(\gamma) < d_{\Omega_i}(\gamma)$ for $\gamma > \gamma_{i+1}^*$ and $d_{\Omega_{i+1}}(\gamma) > d_{\Omega_i}(\gamma)$ for $\gamma < \gamma_i^*$. Operating modes for which these conditions do not hold are irrelevant because either one or both are not active in the solution to (2) or they are over a negligible range of SNRs. The same argument carries on to pathological configurations of the channel codec that fails to realize the best achievable performance (for example if a family of RCPC codes does not use the best puncturing tables). As Figure 2 illustrates, this means that the overall D-SNR curve is the sequential interlacing of sections of single-mode D-SNR curves. These sections are the portion of single-mode D-SNR curves where channel-induced distortion is such that $D_S(\Omega_{i+1}) \leq d_{\Omega_{i+1}}(\gamma) \leq D_S(\Omega_i)$, approximately. Note that these observations follow from the mechanics associated with problem (2), they can be found in applications of this problem with setups very different from the one we are considering [22], [23], [34]. Also note in Figure 2, that at very low SNR (and large distortion) there is an operating region where the smallest of the channel codes has already been chosen and there is no more use of JSCC bit rate allocation. Performance in this region follows that of a system with fixed channel coding, thus it is of no interest to us.

A challenge in studying the D-SNR curves resulting from JSCC bit rate allocation using practical source and channel

coders is that the expressions that could be derived do not lead to a closed form solution to (2). This is true even when resorting to approximations using error exponents for channel codes [40], [41]. Consequently, we study the D-SNR curve through an approximate curve determined by a subset of its points. Each of these points is selected from a different single-mode D-SNR curve. The point selected from some single-mode D-SNR curve $i+1$, must belong to the section that is part of the solution to (2), i.e. it must follow $D_S(\Omega_{i+1}) \leq d_{\Omega_{i+1}}(\gamma) \leq D_S(\Omega_i)$, approximately. This means that a point associated to a small relative contribution of channel errors to the end-to-end distortion is likely to belong to the overall D-SNR curve. Points with a relative contribution of channel errors that is practically negligible or is large may or may not belong to the D-SNR curve and, thus, are not good choices to form the approximation. Then, for each single-mode D-SNR curve, the point chosen to represent the D-SNR curve is such that $d_{\Omega_i}(\gamma) = (1+\Delta)D_S(\Omega_i)$, $\forall \Omega_i$, where Δ is an small number that accounts for the relative contribution of channel errors. Formally, all points such that

$$\begin{aligned} D(\gamma) &= (1+\Delta)D_S(\Omega_i) \\ &= D_F P_{\Omega_i}(\gamma) + D_S(\Omega_i)\Big(1 - P_{\Omega_i}(\gamma)\Big), \end{aligned} \quad (3)$$

form the overall D-SNR curve. Equivalently, from (3), the D-SNR curve is formed by those points where the probability of post-channel decoding errors is

$$P_{\Omega_i}(\gamma) = \frac{\Delta}{\frac{D_F}{D_S(\Omega_i)} - 1}. \quad (4)$$

The advantage offered by (4) is that it simplifies the D-SNR curve characterization problem by translating it into a problem essentially in error control coding. Furthermore, in solving this problem we would also be able to use the fact that channel-induced errors are relatively few, and thus apply approximations that are accurate in the low BER regime. Using this approach, we will show next that, in the region of JSCC bit rate allocation, the D-SNR curve can be closely approximated by

$$D(\gamma) \approx (G_c \gamma)^{-10m}. \quad (5)$$

This expression has the appeal of being of the same form as the error rate-SNR function commonly found in the study of communication systems [1]. The main differences are that we consider distortion instead of average error probability, there is no assumption of asymptotically large SNR, and that (5) will model performance of systems with practical components instead of being a bound. Following this similarity, we can draw the analogy that G_c is the coding gain and m is the diversity gain. The coding gain is the SNR value for which the distortion reaches a reference value of 1. The diversity gain is the slope (i.e. rate of change) of the D-SNR curve when plotted in log-log scales, and it extends the concept of diversity beyond the one limited to the presence of multiple channels or fading. Note that the factor of 10 multiplying m is used so that m is the slope when SNR is measured in dBs. In what follows, the subscript dB will denote any magnitude expressed in decibels, e.g. $\gamma_{dB} = 10\log(\gamma)$.

The derivation of (5) involves finding a relation between distortion and channel SNR. The first step in doing so is the approximation of the D-SNR curve by choosing the subset of points that leads to (4). As this translates the problem into one essentially in error control coding, it becomes possible to apply many of the techniques from error control performance analysis. After recognizing this, the next step in deriving (5) is to write the expression that relates the frame error probability with channel SNR. This relation is normally expressed using some parameters that specify the error correcting capability of the channel code (for example, the minimum distance). Then, the next step is to translate the relation between frame error probability and SNR into one between source encoding rate and SNR. This is achieved by using (4), following by applying an expression that relates the parameters that specify the error correcting capability with the channel coding rate. The expression that is applied here, which would likely be drawn from the error control performance analysis theory, is normally a function that implicitly converts the discrete set of channel rates into a continuous one (this has the extra advantage of minimizing the impact of neglecting bit padding when choosing the active operating modes). Next, the channel coding rates are converted into source encoding rate by applying the definitions of the operating modes and, finally, the relation between source encoding rate and SNR is translated into a function relating SNR with distortion by using (2). Due to the nature of this derivation, the proof of (5) will be dependent on the error performance characterization of the family of channel codes in use. As a representative illustration, we will consider systems using RCPC codes [38], [39] and Reed-Solomon block codes [42] because they can represent a large class of practical designs. We conjecture that our results could also be applicable to other schemes using channel codes not in the class represented by RCPC and RS codes but with an error performance characterization that still show many similarities, yet a proof of this is the subject of future works.

A. RCPC Channel Codes Case

Let channel coding be implemented using a family of RCPC codes. In this case, we can approximate the probability of a source block with post-channel decoding errors as, [43],

$$P(\gamma) \approx 1 - \left(1 - \sum_{d=d_f}^{\infty} a(d) P_e(d|\gamma)\right)^{Nx}, \quad (6)$$

where d_f is the free distance of the code and $a(d)$ is the number of errors events with Hamming weight d and probability of occurrence $P_e(d|\gamma)$. In the special case of BPSK modulation, $P_e(d|\gamma) = .5\ \mathrm{erfc}\sqrt{d\gamma}$ [38], where $\mathrm{erfc}(\gamma)$ is the complementary error function $\mathrm{erfc}(\gamma) = 2/\pi \int_{\gamma}^{\infty} e^{-u^2} du$. Other popular modulation schemes can be represented by a similar form, i.e., a weighted complementary error function with the square root of the SNR as a factor in the argument. As a representative example, we will restrict ourselves to BPSK in what follows. Equation (6) follows from a bound that is tight at low BER operation. In this regime it can be assumed that most errors events are those with $d = d_f$, in which case

(6) can be written as

$$P(\gamma) \approx 1 - \Big(1 - \frac{a(d_f)}{2}\ \text{erfc}\sqrt{d_f \gamma}\Big)^{Nx}. \quad (7)$$

As detailed in Appendix A, it follows from (7) that $\gamma_{dB}(x) \approx A_1 x + B_1$, or, equivalently, $x \approx A_2 \gamma_{dB} + B_2$. Since $D(\gamma) = (1+\Delta)D_S = \mu(1+\Delta)2^{-2\nu x}$, we have

$$\begin{aligned} D(\gamma) &= \mu(1+\Delta)10^{-\nu(\log 4)x} \\ &\approx \mu(1+\Delta)10^{-\nu(\log 4)\left(A_2\gamma_{dB}+B_2\right)} \\ &= \mu(1+\Delta)10^{-\nu B_2(\log 4)}\gamma^{-10\nu A_2 \log 4}. \end{aligned}$$

This is a relation of the form $D(\gamma) \approx (G_c\gamma)^{-10m}$ with, from (28) in Appendix A,

$$m = \frac{\nu \log(4)}{A_1} = \frac{\nu}{10}\left(\frac{cN}{W\ln(4)} + \frac{\nu}{\Psi}\right)^{-1}, \quad (8)$$

$$\begin{aligned} G_c &= \big[\nu(1+\Delta)\big]^{-1/(10m)}10^{-B_1/10} \\ &= \frac{\kappa}{\Psi\big[\nu(1+\Delta)\big]^{1/(10m)}}\Big(\frac{D_S(\bar{x})}{D_F}\Big)^{1/\Psi}, \end{aligned} \quad (9)$$

where $\Psi = \ln\big(\frac{\bar{a}ND_F\bar{x}}{2\Delta D_S(\bar{x})}\big)$, $\bar{x}$ is the average source encoding rate, $\bar{a}$ is the average of $a(d)$ and c and κ are parameters related to d_f of the family of RCPC codes being used. Also, we have used the fact that when no source encoded bits are available at the decoder we have $D_S(0) = \mu \equiv D_F$. Note that, per (8) and (9), the D-SNR performance is now expressed as a function of parameters of the system (such as W and N), the source encoding process (such as ν and μ), the channel encoding process (such as κ and $\bar{a}$) and the parameter from the approximating process Δ.

B. Reed-Solomon (RS) Channel Code Case

Let the channel coding be implemented using a family of RS codes operating on b-bit symbols and with parameters (n,k), i.e. the encoder operates at a rate $r = k/n$, encoding k symbols into an n-symbol codeword. The channel code rate is controlled through the choice of k. Let $L = \frac{W}{nb}$ denote the number of codewords in the frame at the output of the channel encoder. The probability of having a source block with post-channel decoding errors is $P(\gamma) = 1-\big(1-q(\gamma)\big)^L$, where $q(\gamma)$ is the probability of channel decoder failure. Assuming the use of a bounded distance decoder and denoting $l = \lfloor\frac{n-k}{2}\rfloor$, we have $q(\gamma)$ approximated as [42],

$$\begin{aligned} q(\gamma) &= P\Big[\text{codeword symbols in error} > l\Big] \\ &= \sum_{j=l+1}^{n}\binom{n}{j}P_s^j(1-P_s)^{n-j}, \end{aligned} \quad (10)$$

where P_s is the probability of a symbol error. For b-bits symbols, $P_s(\gamma) = 1 - \big(1-P_b(\gamma)\big)^b$, where P_b is the bit error probability, which depends on the modulation and the channel conditions. Considering that P_s and $q(\gamma)$ are small numbers because we are assuming operation in the low BER regime, we can use a first order Taylor's series to approximate $P_s(\gamma) \approx bP_b(\gamma)$, $1-\big(1-q(\gamma)\big)^L \approx Lq$ and assume that the first term in (10) accounts for most of q's magnitude, which means that

$$P(\gamma) \approx L\binom{n}{l+1}P_s^{l+1}(1-P_s)^{n-l-1}. \quad (11)$$

Appendix B shows that from this relation we can write $\gamma_{dB} \approx A_1 x + B_1$. Following the same steps as for RCPC channel codes, we reach the conclusion that $D(\gamma) \approx (G_c\gamma)^{-10m}$ with,

$$m = \frac{W\log(4)}{t_1(0.5)N}, \quad G_c = (1+\Delta)^{-1/(10m)}\frac{10^{t_1(0.5)/20}}{\ln(f(0.5))}, \quad (12)$$

where $f(r)$ and $t_1(r)$ are from (37) and (38) in Appendix B. Finally, note again that the D-SNR performance is now expressed as a function of parameters of the system, the source encoding process, the channel encoding process and the parameter from the approximating process Δ.

TABLE I
VALUES OF $G_{c_{dB}}$ AND m FROM FIGURE 3

Curve	$G_{c_{dB}}$	m
D-SNR curve, RS code, b=5	0.05	0.49
Approximate solution, RS code, b=5	0.12	0.47
D-SNR curve, RS code, b=4	-0.38	0.43
Approximate solution, RS code, b=4	-0.46	0.43
D-SNR curve, RCPC code, M=8	7.29	0.24
Approximate solution, RCPC code, M=8	7.35	0.25
D-SNR curve, RCPC code, M=4	5.71	0.24
Approximate solution, RCPC code, M=4	5.66	0.23

C. Illustration

We illustrate now how the proposed framework accurately characterizes the D-SNR curve. For illustrative purposes we set $\mu = \nu = 1$, which corresponds to assuming that the input signal samples follow a standard Gaussian distribution and that long block source codes are used. For this source model, and assuming that the error concealment replaces each lost sample by its expected value, $D_F = 1$ because the mean squared error equals the variance of each sample.

It will be useful to realize that, since we have observed a linear relation in a log-log scale between D and γ, it is possible to obtained accurate values for m and $G_{c_{dB}}$ from the knowledge of only two points of the D-SNR curve. Let (D_1, γ_{dB1}) and (D_2, γ_{dB2}) be the coordinates of these points. Then,

$$m = \frac{\log\big(D_1/D_2\big)}{\gamma_{dB2} - \gamma_{dB1}}, \quad (13)$$

$$G_{c_{dB}} = -\Big(\gamma_{dB1} + \frac{\log D_1}{m}\Big) \quad (14)$$

The coordinates of these points follow from considering that they are the solution of $D_F P_{\Omega_i}(\gamma) + D_S(\Omega_i)\big(1-P_{\Omega_i}(\gamma)\big) \approx (1+\Delta)D_S(\Omega_i)$. Therefore, denoting the operating modes associated with each of the two points as Ω_1 and Ω_2, the point coordinates in (13) and (14) can be approximated as

$$\begin{aligned} &D_i = \Big(1+\Delta\Big)D_S(\Omega_i), \\ &\gamma_{dBi} = 10\log\Big[P_{\Omega_i}^{-1}\Big(\tfrac{\Delta}{D_F/D_S(\Omega_i)-1}\Big)\Big], i = 1,2 \end{aligned} \quad (15)$$

We now consider systems using RS and RCPC codes.

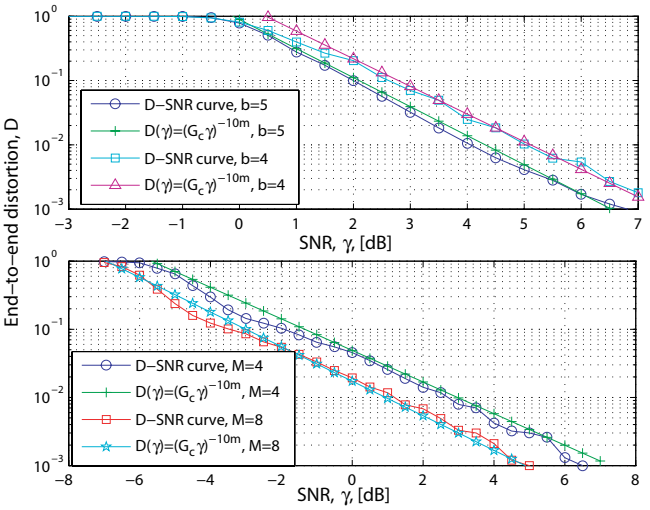

Fig. 3. Application of the proposed framework to systems with different RS (top) and RCPC (bottom) codes.

Figure 3 (top) shows the D-SNR curve, and the corresponding characterizations (5), for two systems using $b = 4$ and $b = 5$ RS codes. For the D-SNR characterization curves, the points (D_1, γ_{dB1}) and (D_2, γ_{dB2}) were found by combining (11) into (15) and solving numerically for γ. We set $N = 150$ samples, $W = 950$ bits, and, for reasons that will be explained in the next section, $\Delta = 0.1$. We choose single-mode D-SNR curves with channel coding rate approximately $r = 1/2$ and $r = 2/3$. Table I shows $G_{c_{dB}}$ and m obtained for both curves. The results show an overall good representation of these parameters and the D-SNR curve. Keeping the same setup as with RS codes, we considered RCPC codes with two families: a memory $M = 8$, [39], and a memory $M = 4$, [38], family. Both families are based on a mother code with rate $1/4$ and puncturing period 8. Figure 3 (bottom) shows the curves obtained using the proposed approach and the D-SNR curves obtained from Monte-Carlo simulation of each single-mode D-SNR curve. The points (D_1, γ_{dB1}) and (D_2, γ_{dB2}) were found by combining (22), from Appendix A, into (15). The D-SNR curves are not as smooth as those for RS codes because the possible channel coding rates in a family of RCPC codes are more concentrated at lower rates. Also, since the complexity of the Viterbi algorithm grows exponentially with the memory of the code, the proposed approach has the key advantage of providing a method that does not requires lengthy Monte-Carlo simulations. Table I shows $G_{c_{dB}}$ and m obtained from Figure 3 (bottom). The results again show an overall good representation of these parameters and the D-SNR curve.

D. Choice of Δ and Its Influence on Results

Since the above results depend on the value chosen for Δ, it is important to study how this choice affects $G_{c_{dB}}$ and m. Thus, we calculate the relative change in $G_{c_{dB}}$ and m as a function of a change in Δ, denoted by δ. Denoting these results as S_G^Δ and S_m^Δ, respectively, they equal

$$S_m^\Delta \triangleq \left(\frac{m(\Delta+\delta)-m(\Delta)}{\delta}\right)\left(\frac{\Delta}{m(\Delta)}\right),$$
$$S_G^\Delta \triangleq \left(\frac{G_{c_{dB}}(\Delta+\delta)-G_{c_{dB}}(\Delta)}{\delta}\right)\left(\frac{\Delta}{G_{c_{dB}}(\Delta)}\right). \quad (16)$$

TABLE II
RELATIVE DEVIATION OF $G_{c_{dB}}$ AND m TO 100% CHANGE IN Δ.

Setup	S_G	S_m
RCPC, M=4	0.01	0.008
RCPC, M=8	0.01	0.0053
RS, b=4	.009	.12
RS, b=5	.006	.07

By examining Figure 2, it is clear that Δ cannot be chosen to be large or very small, since the corresponding distortion points may not belong to the D-SNR curve. Then, we do the study by choosing a reasonable value for Δ (equal to 0.1) and then calculating S_G^Δ and S_m^Δ for relatively large changes in Δ. Table II shows the results for different setups when Δ is assumed to be changed by 100%. The results show that $G_{c_{dB}}$ and m will exhibit little relative deviation to changes in the value of Δ, as long as it follows the above guidelines. Only $G_{c_{dB}}$ when using RS codes show relative deviations larger than 1%, albeit still much smaller than 100 %. This is because the actual values $G_{c_{dB}}$ in these cases are close to 0, which also means that the actual absolute change in $G_{c_{dB}}$ is only tenths of dBs (this can be confirmed with the results in Table I). By examining the formulation in Section III-C and Appendices A and B, it can be seen that any change in δ will have a small effect in changing γ_{dB_1} or γ_{dB_2}. In practical terms, this means that by choosing Δ we are considering points in the "elbow" region of the single-mode D-SNR curves where distortion starts to rapidly increase due to channel-induced errors. In this section, relatively large changes in distortion translates in small changes in γ_{dB}. This is one of the reasons why the subset of points chosen to approximate the D-SNR curve is effective. The other is that, as argued for early in this Section, choosing Δ so that we are considering points in the "elbow" region of the single-mode D-SNR curves (where the contribution of channel-induced distortion is small) ensures that these points either belong to or are close to the D-SNR curve. Therefore, our results here show that Δ have to be chosen to be a small number that corresponds to the "elbow" region of the single-mode D-SNR curves. When doing so, the results show little relative deviation to changes in the value of Δ. Because of these reasons we have chosen Δ around 0.1.

IV. APPLICATIONS OF THE FRAMEWORK

A. Assessing Performance Improvement when Changing Channel Code

The proposed framework is useful in modeling performance effects due to changes in channel coding without the need for lengthy simulations. The performance difference between two schemes could be quantified through the ratio m_1/m_2 and the difference $G_{c_{dB}1} - G_{c_{dB}2}$. Considering the RS codes from Section III-C and using the suffix "1" and "2" to denote the systems with $b = 5$ and $b = 4$ codes, respectively, we get $G_{c_{dB}1} - G_{c_{dB}2} = 0.58$ dB and $m_1/m_2 = 1.09$ from the results using (13), (14) and Table I. These results are close to the actual values $G_{c_{dB}1} - G_{c_{dB}2} = 0.43$ dB and $m_1/m_2 = 1.14$. For the RCPC codes discussed in Section III-C we measured (using Table I) $G_{c_{dB}1} - G_{c_{dB}2} = 1.69$ dB and $m_1/m_2 = 1.08$, while Monte-Carlo simulations yields $G_{c_{dB}1} - G_{c_{dB}2} = 1.58$

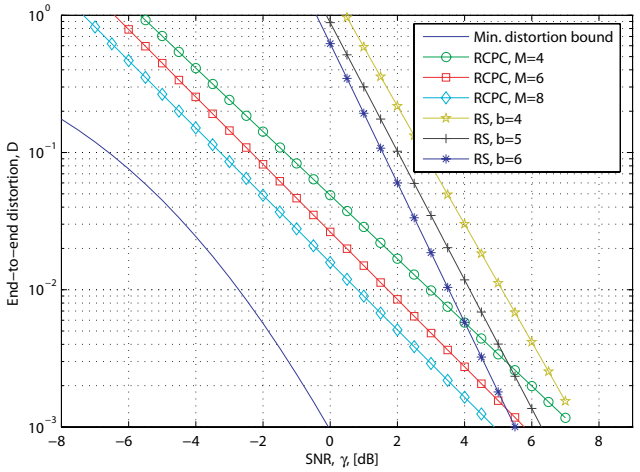

Fig. 4. Comparison between the considered schemes and minimum distortion bound.

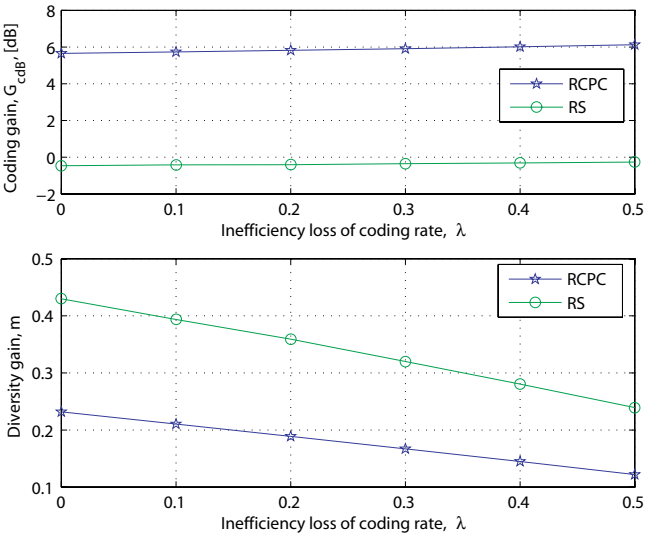

Fig. 5. Coding gain and diversity gain for systems using source codecs with different compression efficiency.

dB and $m_1/m_2 = 1$. In these results the suffixes "1" and "2" denotes the systems with $M = 8$ codes and with $M = 4$ codes, respectively. Incidentally, we note that these results show the accuracy and usefulness of the approximation for the free distance of RCPC codes used in Appendix A, which has not been found in previous published work.

Importantly, these results are useful in providing a simple performance measure for the JSCC bit rate allocation schemes. We illustrate this point by comparing the results with the *minimum distortion bound*, which is the D-SNR curve for a system where the conditions for Shannon's separation principle hold and where the channel is used at its capacity. Following Goblick's approach [44], the minimum distortion bound can be found by simply equating channel capacity to coding rate and applying this value in Equation (1). This bound is shown in Figure 4 along with the approximate D-SNR curves corresponding to systems using different RS and RCPC codes. As is to expect, the use of stronger error correcting codes achieves a performance closer to the minimum distortion bound, yet the figure also shows the difference between the bound and systems with practical constraints for multimedia real-time communication such as delay and system complexity. Also the figure shows a difference in the behavior of systems using RS and RCPC codes. While systems using RCPC codes show changes mostly in coding gain, those using RS codes show changes in coding and diversity gain. This difference is consistent with our expanded view of diversity since the strength of different RCPC codes is controlled by changing their memory, which does not affect the number of redundancy bits sent. For RS codes, the strength is controlled by changing the number of bits per symbols which does change the number of parity symbol sent (for a fixed channel coding rate). These types of observations, which are useful at system design time, show the usefulness of the proposed framework.

B. Assessing Performance as a Function of Source Codec Efficiency

Our previous setting $\mu = \nu = 1$ implicitly assumes that the source encoder is able to compress the input samples perfectly. In reality, different source codecs exhibit different compression efficiency, meaning that same distortion values are achieved at different encoding rates. The efficiency of the source codec can be explicitly incorporated into the formulation by writing the D-R function as $D_S(x) = 2^{-2(1-\lambda)x} = 2^{-\hat{\lambda}x}$, where λ determines the inefficiency as a coding rate loss and $\hat{\lambda} \triangleq 2(1-\lambda)$. By modifying (15) accordingly, i.e. $D_i = (1+\Delta)2^{-\hat{\lambda}x_i}$, $\gamma_{dBi} = 10\log\left[P_{\Omega_i}^{-1}\left(\frac{\Delta}{2^{\hat{\lambda}x_i}-1}\right)\right]$, we studied in Figure 5 the effects of source codec efficiency on the performance.

In Figure 5 we can see that the source coding efficiency has little effect on coding gain. Essentially, this is due to the same reasons why the system shows little relative deviation to changes in Δ. To understand this, consider firstly that it is possible in (14) to accurately approximate $\log(D_1) \approx \log(D_S(x_1))$. Secondly, as was the case for Δ, it can be seen in the formulation in Section III-C and Appendices A and B that λ would have little effect on γ_{dB} (this is more clear for RCPC codes). In contrast, larger source encoder efficiencies translate into greater diversity gains because, since λ has little effect on γ_{dB}, we can see from (13) that changes in m are proportional to $\hat{\lambda}$. This point can be verified in Figure 5 by testing any ratio of two diversity gains. These observations are consistent with our expanded view of diversity because the reduction in source codec efficiency translates into sending less redundant error correction data for a fixed end-to-end distortion.

C. Application to Speech Communication over CDMA Cellular Network

Since our approach is based on sufficiently general dynamics of the JSCC bit rate allocation problem, we conjecture that it can be applied to many other schemes that do not need to follow all of our initial assumptions. Next, we highlight this point by considering a setup that only follows our assumption for practical channel codes. Specifically, we will consider that the source is speech, which is encoded with a

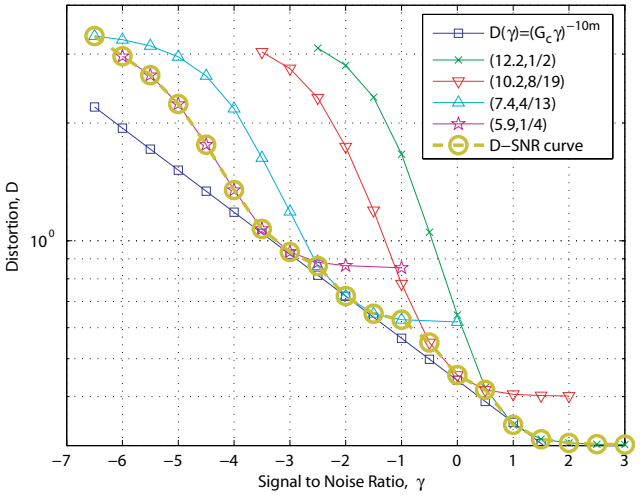

Fig. 6. Joint source-channel bit rate allocation for a CDMA speech communication system.

practical and widely-used speech vocoder (the GSM AMR codec [45]). Also, distortion is now measured differently, using a perceptually-based measure that is intimately related to the ITU-T PESQ quality measure standard P.862 [46]. PESQ is an algorithm that produces measurements of quality as numbers between 4.5 and 1 [47], where higher values means better quality. The most important property of PESQ is that its results accurately predict those that would be obtained in a typical subjective test using the method of polling a panel of human listeners (the MOS test [48]).

Consider the uplink of a CDMA cell carrying real-time speech traffic. For illustrative purposes assume that the transmit bit rate is kept fixed at 24.4 Kbps (fixed processing gain system) and the channel code is the memory 4, mother code rate $1/4$, RCPC code family from [38]. We allow four possible operating modes. Specifying the modes by the pair (source coding rate, channel coding rates), the possible choices are: $(12.2$ Kbps$, 1/2)$, $(10.2$ Kbps$,8/19)$, $(7.4$ Kbps$, 4/13)$ and $(5.9$ Kbps$, 1/4)$. Figure 6 shows the single-mode and the overall D-SNR curves. Each single mode D-SNR curve was obtained through Monte Carlo simulations with 18 different speech sequences (both male and female speakers) from the TIMIT speech corpus [49] and 50 simulation runs. The simulations included the use of the error concealment option of the source codec. Distortion was measured as $4.5 - Q$, where Q is the result of the PESQ algorithm. Figure 6 shows that the approximation (5) is very good over the range of the Signal-to-Interference-plus-Noise ratio (SINR) where JSCC bit rate allocation is used. This observation, highlighted by the fact that there are very few coincidences between the current setup and the one assumed in Section II, suggests that the proofs in Section III could be extended to other setups and our framework be applied in a wide range of applications.

Both the processing and the coding gains can be calculated from the formulas already developed with minimal changes. In (3), D_F is the distortion when the speech decoder applies error concealment. In the present case we simply assume a worst case scenario $D_F = D_{max} = 3.5$. Of course, including a more accurate model for D_F could only improve our results, but this is not the focus of this paper. Also, we do not assume any particular model for the source-encoded distortion $D_S(x_i)$, we just assumed the value is known from the codec design specifications. Thus, the two point coordinates used to find m and $G_{C_{dB}}$ are $((1+\Delta)D_S(x_1), \gamma_{dB1})$ and $((1+\Delta)D_S(x_2), \gamma_{dB2})$, with γ_{dB1} and γ_{dB2} calculated by modifying Equation (22) in Appendix A as

$$\begin{aligned}\gamma_{dB} &= 20\log\left(\operatorname{erfc}^{-1}\left(\frac{2}{\bar{a}}\left[1-\left(1-\frac{\Delta}{\frac{3.5}{D_S(\Omega_i)}-1}\right)^{1/x}\right]\right)\right) \\ &- 10\log\kappa + 10cWx\log e, \end{aligned} \tag{17}$$

where x is the source encoding rate per transmission period, i.e. the source encoding rate for each operating mode times $20ms$ (the duration of a transmission period). We highlight that to apply our framework it is necessary to only know parameters from the source and the channel codecs that are determined at their design times. In contrast, to find each point of the D-SNR curves in Figure 6 it was necessary to perform 1900 simulation runs. We also note that because we assume availability of only 4 modes, the interlacing between each single mode D-SNR curve is much coarser than the one shown in Figure 2. Since the effect of interlacing single-mode D-SNR curves was used to derive our framework, it is interesting to note that even when the interlacing is coarse the framework still approximates well the overall D-SNR curve.

To illustrate how this result can be used in the study of a design, assume a system with U users, BPSK modulation, ideal power control, a matched filter at the receiver and AWGN background noise with variance σ^2. It can be shown that at the receiver, the power assigned to user i to transmit a frame, P_i, is related to the target SINR, γ_i, by [50], [51],

$$P_i = \frac{\Upsilon_i \sigma^2}{1 - \sum_{j=1}^{U} \Upsilon_j}, \quad i = 1, 2, \cdots, N. \tag{18}$$

where $\Upsilon_i = \left(1 + \frac{G_P}{\gamma_i}\right)^{-1}$ and G_P is the processing gain (equal to system bandwidth over transmit bit rate). From (18), constraints on positive power assignments and system stability results in the limit to the number of user given by the condition

$$\sum_{i=1}^{U} \left(1 + \frac{G_P}{\gamma_i}\right)^{-1} = 1 - \epsilon, \tag{19}$$

where ϵ is a small positive number set during design.

It is easy to show that assigning the same target SINRs to all calls is optimal for the present setup [51]. Therefore, from (19), target SINR and number of voice calls are related by,

$$\gamma = \frac{G_P}{\frac{U}{1-\epsilon} - 1}. \tag{20}$$

Combining this result with (5) and performing some algebraic operations yields $U = (1-\epsilon)\left[1 + D^{1/10m} 10^{(G_{C_{dB}} + G_{P_{dB}})/10}\right]$, which is useful in that it relates the number of calls with the end-to-end distortion in a simple way that uses four simple system parameters: ϵ and $G_{P_{dB}}$ from the CDMA network design, and $G_{C_{dB}}$ and m from the JSCC bit rate allocation design. Our framework shows now it usefulness since all the above studies can be applied to this problem, allowing straightforward analysis of how the CDMA network behavior would change with different source or channel coding. Also,

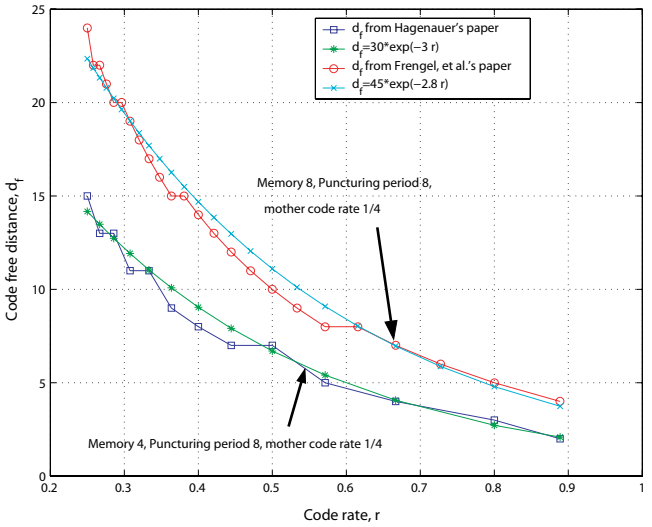

Fig. 7. Code rate vs. free distance for two families of RCPC codes from Hagenauer's [38] and Frengel's [39] papers.

note that our framework reveals that processing gain and coding gain both have the same effect on the CDMA system performance.

V. Conclusions

In this paper we have proposed a unified framework for the modeling and analysis of real-time multimedia systems. This framework is based on a general view of diversity that is not limited to the presence of multiple channels or fading, and that includes redundancy as an instance of diversity. We show that the D-SNR curves resulting from solving the JSCC bit rate allocation problem for a certain range of multimedia systems can be accurately represented as $D(\gamma) \approx (G_C\gamma)^{-10m}$. Recognizing the linear behavior in log-log scale of this function and its similarity to the error rate-SNR expressions in data transmission systems, we named G_c the coding gain and m the diversity gain. This result allows measuring and comparing performance of JSCC multimedia schemes with a representation in unison with the one used for traditional diversity.

In our presentation we have explained why and how the D-SNR curve can be characterized by a subset of points where the relative contribution of channel errors to the end-to-end distortion is fixed and small (mathematically, $D(\gamma) \approx (1+\Delta)D_s$). This is the basis of our approach, which avoids the use of information-theoretic analysis such as assuming infinite complexity and delay, and which results in a tight and simple approximation to the D-SNR performance curves for systems with practical multimedia sources, source codecs and channel codecs. The proposed approach allowed us to quantify how performance changes when a stronger channel code is used and the performance difference between practical systems and an ideal information-theoretical bound. Also, by using the proposed approach we were able to study and measure the different behavior between block and convolutional codes and we related the results to the unifying view of diversity. In addition, we also study and measure the effects that the efficiency of the source codec has on system performance and we show that it affects only the diversity gain (not the coding gain) reducing it proportionally to the codec loss of efficiency. Also, as a side contribution, we presented a useful relation that links error performance with channel coding rate in families of RCPC codes.

We have characterized the D-SNR curve for systems using RCPC and RS codes. These codes were chosen due to their popularity in multimedia systems with variable-rate channel coding and as representatives of a large class of channel codes that share the same performance characterization (e.g. block channel codes), to which our approach can also be applied. Then, we believe that our approach could be used to characterize a wide range of practical JSCC multimedia systems. This is emphasized by showing the accuracy of the proposed approach when applied to a CDMA network carrying speech calls encoded with the GSM-AMR codec and distortion measured with the perceptually-based PESQ standard. Based on its simplicity, flexibility and accuracy, the proposed approach opens the possibility of studying other JSCC systems from a new and important viewpoint.

Appendix

A. Channel SNR as a function of source encoding rate for RCPC codes

In this appendix we show that the channel SNR can be approximated as $\gamma_{dB} \approx A_1 x + B_1$ for RCPC codes. First, consider that Equation (7) shows an implicit dependence, through d_f and $a(d_f)$, between $P(\gamma)$ and the rate of the channel code, i.e. the particular operating mode. To make this dependence explicit, we study next the relation between d_f and $a(d_f)$ with r. Figure 7 shows how d_f changes as a function of the code rate r for two representative RCPC codes families: one from [38] and the other from [39]. It can be seen that the free distance can be approximated by a function of the form $d_f \approx \kappa e^{-cr} \approx \kappa e^{-cNx/W}$, where κ and c are two constants. A similar study for $a(d_f)$ shows that it is not possible to find a practical functional approximation. Therefore, we will roughly approximate $a(d_f)$ by taking its average value , $\bar{a} = \sum_\pi a_\pi(d_f)/|\pi|$, where π is an index into each of the members of the family of RCPC codes used for error protection and $|\pi|$ is the number of codes in the family. This approximation will prove to yield good results. Using the approximations for d_f and $a(d_f)$, Equation (7) becomes

$$P(\gamma) \approx 1 - \left(1 - \frac{\bar{a}}{2}\,\mathrm{erfc}\sqrt{\kappa e^{-cNx/W}\gamma}\right)^{Nx}. \qquad (21)$$

Using (4), Equation (21) can be solved for γ to show the explicit relation between γ and source coding rate x.

$$\gamma(x) \approx \frac{1}{\kappa} e^{cNx/W} \left(\mathrm{erfc}^{-1}\left(\frac{2}{\bar{a}}\left[1 - \left(1 - \frac{\Delta}{\frac{D_F}{D_S(x)} - 1}\right)^{1/(Nx)}\right]\right)\right)^2. \qquad (22)$$

Equation (22) shows that two factors contribute to γ: the inverse of the free distance and the square of an inverse complementary error function. Let's denote this second factor by $g(x)$. Using the approximation $\mathrm{erfc}^{-1}(y) \approx \sqrt{-\ln(y)}$,

[52], yields

$$g(x) \approx \ln\left(\frac{\bar{a}}{2}\right) - \ln\left(1 - \left(1 - \frac{\Delta}{\frac{D_F}{D_S(x)} - 1}\right)^{1/(Nx)}\right). \quad (23)$$

Before continuing, we note that the approximation $\text{erfc}^{-1}(y) \approx \sqrt{-\ln(y)}$ is not tight, yet it is very good in representing the behavior of the inverse error function, which justifies its use. In essence, this means that the modulation scheme has a probability of error that behaves approximately as e^{-x^2} with respect to SNR. Working with the second term of the right hand side of (23),

$$\theta = -\ln\left(1 - \left(1 - \frac{\Delta}{\frac{D_F}{D_S(x)} - 1}\right)^{1/(Nx)}\right) \quad (24)$$

$$\Rightarrow \ln\left(1 - e^{-\theta}\right) = \frac{1}{Nx}\ln\left(1 - \frac{\Delta}{\frac{D_F}{D_S(x)} - 1}\right) \quad (25)$$

$$\Rightarrow -e^{-\theta} \approx \frac{1}{Nx}\left(-\frac{\Delta}{\frac{D_F}{D_S(x)} - 1}\right) \quad (26)$$

$$\Rightarrow \theta \approx \ln\left(\frac{N}{\Delta}x\left(\frac{D_F}{D_S(x)} - 1\right)\right)$$

$$\approx \ln\left(\frac{N}{\Delta}x\right) + \ln\left(\frac{D_F}{D_S(x)}\right), \quad (27)$$

where (26) follows from the fact that both logarithms in (25) are of the form $\ln(1-y)$ with $y \ll 1$, which can be seen from (24) and (4) considering that $P_{\Omega_i}(\gamma)$ is typically small. The approximation in (27) follows from recognizing that in general $D_F/D_S(x) - 1 \approx D_F/D_S(x)$, i.e. the reconstructed source error after transmission errors is typically much larger than the quantization distortion. From (27), θ is the sum of $\ln(Nx/\Delta)$ and a term that, following (1), is approximately linear in x. Since generally $N/\Delta \gg x$, we can approximate $\ln(Nx/\Delta) \approx \ln(N\bar{x}/\Delta)$, with $\bar{x}$ being the average value of x, and consider that the approximately linear term would determine the overall behavior of $\theta(x)$. Using (1) and (23), it follows that $g(x) \approx \ln\left(\frac{\bar{a}ND_F\bar{x}}{2\Delta\mu}\right) + 2\nu x\ln(2)$. Furthermore, through algebraic operations it can be shown that the coefficients of Taylor's expansion of $\log(g(x))$ around $\bar{x}$ are of the form $t^i/i!$, with $t = \nu\ln(4)\left(\ln(\frac{\bar{a}ND_F\bar{x}}{2\Delta D_S(\bar{x})})\right)^{-1}$ being much smaller than 1 for typical system parameters. This means that the weight of coefficients in Taylor's expansion falls quite rapidly and $\log(g(x))$ can be accurately approximated through a first order expansion. Combining these facts with (22) and (23), and denoting $\Psi = \ln\left(\frac{\bar{a}ND_F\bar{x}}{2\Delta D_S(\bar{x})}\right)$, γ in decibels can be approximated as

$$\gamma_{dB}(x) \approx \frac{10cNx}{W}\log(e) - 10\log(\kappa) + 10\left(\log(\Psi) + \frac{\nu\log(4)}{\Psi}(x - \bar{x})\right), \quad (28)$$

which is a linear function in x.

B. Channel SNR as a function of source encoding rate for RS codes

In this appendix we show that the channel SNR can be approximated as $\gamma_{dB} \approx A_1x + B_1$ for RS codes. Let

$$a = \frac{n}{l+1} - 1,$$

$$Q = \left(\frac{L}{\Delta}\binom{n}{l+1}\left[\frac{D_F}{D_S(Wr/N)} - 1\right]\right)^{-\frac{1}{l+1}}. \quad (29)$$

Combining (4) and (11) leads to $P_s(1-P_s)^a \approx Q$, which can be approximated as $aP_s^2 - P_s + Q = 0$ by using a Taylor series expansion. This approximation is accurate because P_s is a small number. The second order equation has solution $P_s = (1 - \sqrt{1-4aQ})/(2a)$. Since $P_s \approx bP_b(\gamma)$, we have $b\ \text{erfc}(\sqrt{\gamma}) \approx \frac{1-\sqrt{1-4aQ}}{a}$. Similarly to the RCPC code case, using $\text{erfc}^{-1}(y) \approx \sqrt{-\ln(y)}$, yields

$$\gamma \approx \ln\left(ba\right) - \ln\left(1 - \sqrt{1-4aQ}\right) \quad (30)$$

Stirling's formula $n! \approx \sqrt{2\pi n}(n/e)^n$ can be used to approximate factorials (error is less than 4 % for $n > 1$, and decreasing in n) and to write the binomial coefficient in Q as shown in (31). Then we have (32), (33), and (34), where the approximation (32) follows from neglecting the terms equal to one in $l+1$, $n-l-1$ and $\frac{D_F}{D_S(Wr/N)} - 1$, and by setting $l(n-l)/n = n(1-r^2)/4$. This last equality is because $l = \lfloor\frac{n-k}{2}\rfloor = \frac{n-k}{2} = \frac{1-r}{2}$, which follows from the fact that in order for each value of k to yield a different error performance, it is best to choose k of the same type odd/even as n. While the approximations in (32) have a negligible effect, the approximation in (33) changes the value of $4aQ$ by adding a small constant value. Yet, this is not a problem since our goal here is to highlight the functional relations with r, which is maintained in (33). Also, in (34) we have used (1) and the fact that when there are uncorrected channel errors we have $D_S(0) = \mu \equiv D_F$. Next, to simplify notation let's denote

$$h(r) = \left(\frac{1+r}{2}\right)^n\sqrt{\frac{\pi}{2}n}\frac{\Delta}{L}2^{-2\nu Wr/N}, \quad (35)$$

$$u(r) = 1 - 4h(r)^{\frac{2}{n(1-r)+2}}, \quad (36)$$

$$f(r) = \frac{b^{\frac{n-l-1}{l+1}}}{1 - \sqrt{u(r)}} \approx \frac{b^{\frac{n-l}{l}}}{1 - \sqrt{u(r)}} \approx \frac{b^{\frac{1+r}{1-r}}}{1 - \sqrt{u(r)}}. \quad (37)$$

Consider Taylor's series for $\gamma_{dB}(r) = 10\log(\ln(ba) - \ln(1 - \sqrt{1-4aQ}))$ around $r = 0.5$. Figure 8 shows, on top, $\gamma_{dB}(r)$ for different RS codes and their approximations using Taylor's first order series around $r = 0.5$. It can be seen that the approximation is quite good for channel coding rates up to approximately $3/4$. Channel codes rates much larger than this value are not normally seen in practice because, given the complexity and weakness of high rate codes, the choice is frequently to leave the system uncoded. Furthermore, the bottom of Figure 8 shows that the contribution of higher order terms decreases rapidly and never exceeds 10% of the magnitude of the first order approximation. This can be shown to be due to the rapid decrease in the weight of the factors $(r - 0.5)^p$, where p is the term order. Therefore, we can approximate $\gamma_{dB} \approx rt_1(0.5) + t_0(0.5) - t_1(0.5)/2$, where $t_0(r) = 10\log(\ln(f(r)))$ and (38). Using $r \approx Nx/W$, it follows that $\gamma_{dB} \approx A_1x + B_1$.

$$\binom{n}{l+1} \approx \frac{\sqrt{n}\; n^n}{\sqrt{2\pi(l+1)(n-l-1)}\;(l+1)^{l+1}\;(n-l-1)^{n-l-1}} \tag{31}$$

$$\begin{aligned}
4aQ &\approx 4\left(\left(\frac{n-l-1}{n}\right)^n \sqrt{\frac{2\pi(l+1)(n-l-1)}{n}}\,\frac{\Delta}{L\left[\frac{D_F}{D_S(Wr/N)}-1\right]}\right)^{1/(l+1)} \\
&\approx 4\left(\left(\frac{n-l-1}{n}\right)^n \sqrt{\frac{\pi}{2}n(1-r^2)}\,\frac{\Delta D_S(Wr/N)}{LD_F}\right)^{1/(l+1)} \qquad (32)\\
&\approx 4\left(\left(\frac{n-l}{n}\right)^n \sqrt{\frac{\pi}{2}n}\,\frac{\Delta D_S(Wr/N)}{LD_F}\right)^{1/(l+1)} \qquad (33)\\
&= 4\left(\left(\frac{1+r}{2}\right)^n \sqrt{\frac{\pi}{2}n}\,\frac{\Delta}{L}2^{-2\nu Wr/N}\right)^{\frac{2}{n(1-r)+2}} \qquad (34)
\end{aligned}$$

$$\begin{aligned}
t_1(r) &= \frac{10f(r)'}{f(r)\ln(f(r))\ln(10)} \\
&= \frac{10/\ln(10)}{\ln(f(r))}\left[\frac{2}{1-r^2}+\frac{1-1/u(r)}{\sqrt{u(r)}[n(1-r)+2]}\left(\frac{n\ln(h(r))}{n(1-r)+2}+\frac{n}{r+1}-\frac{W\ln(4)}{N}\right)\right]. \qquad (38)
\end{aligned}$$

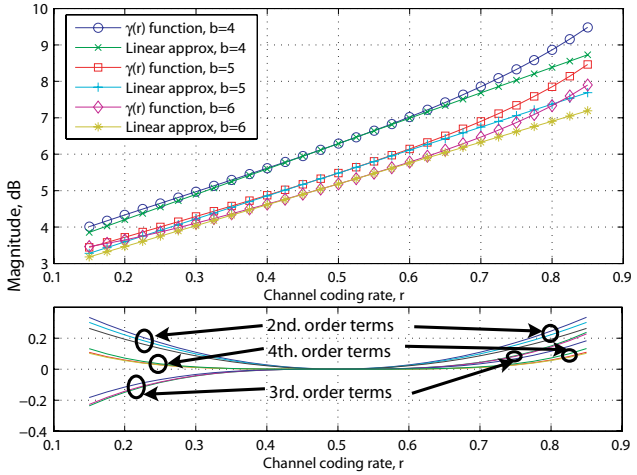

Fig. 8. Top: γ_{dB} as a function of channel coding rate r and its approximation using Taylor's first order series around $r = 0.5$. Bottom: Higher order terms in Taylor's series.

REFERENCES

[1] V. Tarokh, N. Seshadri, and A. R. Calderbank, "Spacetime codes for high data rate wireless communication: Performance criterion and code construction," *IEEE Trans. Inf. Theory*, vol. 44, no. 2, pp. 744–765, March 1998.

[2] J. N. Laneman, E. Martinian, G. W. Wornell, and J. Apostolopoulos, "Source-channel diversity for parallel channels," *IEEE Trans. Inf. Theory*, vol. 51, no. 10, pp. 3518–3539, Oct. 2005.

[3] R. M. Gray and D. L. Neuhoff, "Quantization," *IEEE Trans. Inf. Theory*, vol. 44, no. 6, pp. 2325–2383, Oct. 1998.

[4] N. Demir and K. Sayood, "Joint source/channel coding for variable length codes," in *Proc. Data Compression Conference (DCC)*, April 1998, pp. 139–148.

[5] C. E. Shannon, "A mathematical theory of communication," *Bell Syst. Tech. J.*, vol. 27, pp. 379–423, 1948.

[6] ——, "Coding theorems for a discrete source with a fidelity criterion," *IRE Nat. Conv. Rec.*, pp. 142–163, March 1959.

[7] F. Hekland, G. E. Oien, and T. A. Ramstad, "Using 2:1 Shannon mapping for joint source-channel coding," in *Proc. Data Compression Conference (DCC)*, March 2005, pp. 223–232.

[8] V. A. Vaishampayan and N. Farvardin, "Joint design of block source codes and modulation signal sets," *IEEE Trans. Inf. Theory*, vol. 38, no. 4, pp. 1230–1248, July 1992.

[9] B. Chen and G. W. Wornell, "Analog error-correcting codes based on chaotic dynamical systems," *IEEE Trans. Commun.*, vol. 46, no. 7, pp. 881–890, July 1998.

[10] A. Fuldseth and T. A. Ramstad, "Bandwidth compression for continuous amplitude channels based on vector approximation to a continuous subset of the source signal space," in *Proc. 1997 International Conference on Acoustics, Speech and Signal Processing ICASSP*, vol. 4, pp. 3093–3096.

[11] T. A. Ramstad, "Signal processing for multimedia–robust image and video communication for mobile multimedia," in *NATO Science Series: Computers & Systems Sciences*, vol. 174. IOS Press, 1999, pp. 71–90.

[12] J. M. Lervik and T. A. Ramstad, "Robust image communication using subband coding and multilevel modulation," in *Proc. SPIE Symposium on Visual Communications and Image Processing VCIP*, March 1996, pp. 524–535.

[13] H. Coward and T. A. Ramstad, "Robust image communication using bandwidth reducing and expanding mappings," in *Proc. ASILOMAR Conference on Signals, Systems, and Computers*, Oct. 2000, pp. 1384–1388.

[14] U. Mittal and N. Phamdo, "Hybrid digitalanalog (hda) joint sourcechannel codes for broadcasting and robust communications," *IEEE Trans. Inf. Theory*, vol. 48, no. 5, pp. 1082–1102, May 2002.

[15] M. Skoglundl, N. Phamdo, and F. Alajaji, "Hybrid digital-analog coding for bandwidth compression/expansion using vq and turbo codes," in *Proc. Int. Symp. Inf. Theory*, June 2001, p. 260.

[16] ——, "Vq-based hybrid digital-analog joint source-channel coding," in *Proc. Int. Symp. Inf. Theory*, June 2000, p. 403.

[17] S. Shamai, S. Verdu, and R. Zamir, "Systematic lossy source/channel coding," *IEEE Trans. Inf. Theory*, vol. 44, pp. 564–579, March 1998.

[18] J. G. Dunham and R. M. Gray, "Joint source and noisy channel trellis encoding," *IEEE J. Sel. Areas Commun.*, vol. 27, no. 4, pp. 516–519, July 1981.

[19] N. Farvardin and V. Vaishampayan, "Optimal quantizer design for noisy channels: An approach to combined source-channel coding," *IEEE J. Sel. Areas Commun.*, vol. 33, no. 6, pp. 827–838, Nov. 1987.

[20] K. Zeger and A. Gersho, "Pseudo-gray coding," *IEEE J. Sel. Areas Commun.*, vol. 38, no. 12, pp. 2147–2158, Dec. 1990.

[21] M. Srinivasan and R. Chellappa, "Adaptive source-channel subband

video coding for wireless channels," *IEEE Trans. Inf. Theory*, vol. 16, no. 9, pp. 1830–1839, Dec. 1998.
[22] D. J. Goodman and C. E. Sundberg, "Combined source and channel coding for variable- bit- rate speech transmission," *Bell System Technical J.*, vol. 62, p. 20172036, Sept. 1983.
[23] J. W. Modestino and D. G. Daut, "Combined source-channel coding of images," *IEEE Trans. Commun.*, vol. 27, no. 11, pp. 1644–1659, Nov. 1979.
[24] L. M. Kondi, F. Ishtiaq, and A. K. Katsaggelos, "Joint source-channel coding for motion-compensated dct-based snr scalable video," *IEEE Trans. Image Processing*, vol. 11, no. 9, pp. 1043–1052, Sept. 2002.
[25] A. Goldsmith, "Joint source/channel coding for wireless channels," in *Proc. IEEE 45th Vehicular Technology Conference*, vol. 2, 1995, pp. 614–618.
[26] P. H. Westerink, J. Biemond, and D. E. Boekee, "An optimal bit allocation algorithm for subband coding," in *Proc. 1988 International Conference on Acoustics, Speech and Signal Processing ICASSP88*, pp. 757–760, 1988.
[27] Y. Shoham and A. Gersho, "Efficient bit allocation for an arbitrary set of quantizers," *IEEE Trans. Acoust. Speech, Signal Processing*, vol. 36, no. 9, pp. 1445–1453, Sept. 1988.
[28] P. Ligdas and N. Farvadin, "Optimizing the transmit power for slow fading channels," *IEEE Trans. Inf. Theory*, vol. 46, no. 2, pp. 565–576, March 2000.
[29] A. Kwasinski and N. Farvardin, "Optimal resource allocation for cdma networks based on arbitrary real-time source coders adaptation with application to mpeg4 fgs," in *Proc. IEEE Wireless Communications and Networking Conference (WCNC)*, March 2004.
[30] M. Bystrom and T. Stockhammer, "Dependent source and channel rate allocation for video transmission," *IEEE Trans. Wireless Commun.*, vol. 3, no. 1, pp. 258–268, Jan. 2004.
[31] T. Berger, *Rate Distortion Theory*. Prentice-Hall, 1971.
[32] B. Hochwald and K. Zeger, "Tradeoff between source and channel coding," *IEEE Trans. Inf. Theory*, vol. 43, no. 5, pp. 1412–1424, Sept. 1997.
[33] B. Hochwald, "Tradeoff between source and channel coding on a gaussian channel," *IEEE Trans. Inf. Theory*, vol. 44, no. 7, pp. 3044–3055, Oct. 1998.
[34] M. Bystrom and J. Modestino, "Recent advances in joint source-channel coding of video," in *Proc. 1998 URSI International Symposium on Signals, Systems, and Electronics*, Sept. 1998, pp. 332–337.
[35] A. Kwasinski, "Cross-layer resource allocation protocols for multimedia cdma networks," Ph.D. dissertation, University of Maryland, College Park, MD, 2004.
[36] Z. He, J. Cai, and C. W. Chen, "Joint source channel rate-distortion analysis for adaptive mode selection and rate control in wireless video coding," *IEEE Trans. Circuits Systems Video Technology*, vol. 12, no. 6, pp. 511–523, June 2002.
[37] A. Kwasinski, Z. Han, K. J. R. Liu, and N. Farvardin, "Power minimization under real-time source distortion constraints in wireless networks," in *Proc. IEEE Wireless Communications and Networking Conference (WCNC)*, vol. 1, March 2003, pp. 532–536.
[38] J. Hagenauer, "Rate compatible punctured convolutional (RCPC) codes and their applications," *IEEE Trans. Commun.*, vol. 36, no. 4, pp. 389–399, April 1988.
[39] P. Frenger, P. Orten, T. Ottosson, and A. B. Svensson, "Rate-compatible convolutional codes for multirate ds-cdma systems," *IEEE Trans. Commun.*, vol. 47, pp. 828–836, June 1999.
[40] J. M. Wozencraft and I. M. Jacobs, *Principles of Communication Engineering*. Wiley, 1965.
[41] A. J. Viterbi, "Error bounds for convolutional codes and an asymptotically optimum decoding algorithm," *IEEE Trans. Inf. Theory*, vol. 13, pp. 260–269, April 1967.
[42] S. Wicker, *Error Control Systems for Digital Communication and Storage*. Prentice Hall, 1995.
[43] E. Malkamaki and H. Leib, "Evaluating the performance of convolutional codes over block fading channels," *IEEE Trans. Inf. Theory*, vol. 45, no. 5, pp. 1643–1646, July 1999.
[44] T. Goblick Jr., "Theoretical limitations on the transmission of data from analog sources," *IEEE Trans. Inf. Theory*, vol. 11, no. 4, pp. 558–567, Oct. 1965.
[45] ETSI/GSM, "Digital cellular telecommunications system (phase 2+); adaptive multi-rate (amr) speech transcoding (gsm 06.90 version 7.2.1 release 1998)," in *Document ETSI EN 301 704 V7.2.1 (2000-04)*.
[46] ITU-T, "Recommendation p.862: Perceptual evaluation of speech quality (pesq): An objective method for end-to-end speech quality assessment of narrow-band telephone networks and speech codecs," 2001.
[47] ——, "Recommendation p.862.1: Mapping function for transforming p.862 raw result scores to mos-lqo," 2003.
[48] ——, "Recommendation p.800: Methods for subjective determination of transmission quality," 1996.
[49] D. Timit, "Acoustic-phonetic continuous speech corpus cd-rom," in *Document NISTIR 4930, NIST Speech Disk 1-1.1*.
[50] A. Sampath, N. B. Mandayam, and J. M. Holtzman, "Power control and resource management for a multimedia cdma wireless system," in *Proc. PIMRC'95*, 1995.
[51] A. Kwasinski and N. Farvardin, "Resource allocation for CDMA networks based on real-time rate adaptation," in *Proc. IEEE International Conference on Communications (ICC)*, May 2003.
[52] M. Chiani, D. Dardari, and M. K. Simon, "New exponential bounds and approximations for the computation of error probability in fading channels," *IEEE Trans. Wireless Commun.*, vol. 2, no. 4, pp. 840–845, July 2003.

Andres Kwasinski received in 1992 his diploma in Electrical Engineering from the Buenos Aires Institute of Technology, Buenos Aires, Argentina, and the MS and PhD degrees in Electrical and Computer Engineering from the University of Maryland, College Park, Maryland, in 2000 and 2004, respectively. From 2004 to 2006 he was a Faculty Research Associate in the Department of Electrical and Computer Engineering at the University of Maryland, working on wireless multimedia communications. In addition, he worked during 1993 for NEC as telephone switches software developer and from 1994 to 1998 for Lucent Technologies in several capacities. He is currently with Texas Instruments Inc., DSP Systems. His research interests are in the area of multimedia wireless communications, cross layer designs, digital signal processing and speech and video processing (especially in the area of signal compression).

K. J. Ray Liu (F03) received the B.S. degree from the National Taiwan University and the Ph.D. degree from UCLA, both in electrical engineering. He is Professor and Associate Chair, Graduate Studies and Research, of Electrical and Computer Engineering Department, University of Maryland, College Park. His research contributions encompass broad aspects of wireless communications and networking, information forensics and security, multimedia communications and signal processing, bioinformatics and biomedical imaging, and signal processing algorithms and architectures.

Dr. Liu is the recipient of numerous honors and awards including best paper awards from IEEE Signal Processing Society (twice), IEEE Vehicular Technology Society, and EURASIP; IEEE Signal Processing Society Distinguished Lecturer, EURASIP Meritorious Service Award, and National Science Foundation Young Investigator Award. He also received various teaching and research recognitions from University of Maryland including university-level Distinguished Scholar-Teacher Award, Invention of the Year Award, Fellow of Academy for Excellence in Teaching and Learning, and college-level Poole and Kent Company Senior Faculty Teaching Award.

Dr. Liu is Vice President Publications and on the Board of Governor of IEEE Signal Processing Society. He was the Editor-in-Chief of *IEEE Signal Processing Magazine* and the founding Editor-in-Chief of *EURASIP Journal on Applied Signal Processing*.